The Journal of Neuroscience, January 1994, 14(1): 399–408

Novel Hyperpolarization-activated K^+ Current Mediates Anomalous Rectification in Crayfish Muscle

Alfonso Araque and Washington Buño

Instituto Cajal, CSIC, E-28002 Madrid, Spain

The ionic current underlying anomalous rectification in opener muscle fibers of crayfish was studied under two-electrode voltage clamp. Opener muscle fibers showed a mean resting potential (RP) of −64.8 mV and an input resistance of 0.4 MΩ. Hyperpolarizing voltage command pulses from a holding potential (H) of −60 mV evoked an instantaneous voltage-independent linear current (I_L) followed by a time- and voltage-dependent inward current (I_{AB}) that reached a steady state within 500 msec. The reversal potential of I_{AB} (E_{AB}) was estimated from tail current amplitudes. At an extracellular K^+ concentration ($[K^+]_o$) of 5.4 mM the mean E_{AB} was −61.8 mV. E_{AB} shifted toward positive potentials by 50.8 mV for a 10-fold increase in $[K^+]_o$. The conductance underlying I_{AB} (G_{AB}) increased sigmoidally with hyperpolarization, starting close to the RP, saturating at a $G_{AB,max}$ of about −140 mV, and showing a mean half-activation at −94.4 mV. The activation curve of G_{AB} shifted 53.6 mV toward positive potentials with a 10-fold increase in $[K^+]_o$. $G_{AB,max}$ did not increase in raised $[K^+]_o$. The activation and deactivation kinetics of I_{AB} were accurately described by single exponentials with similar time constants (< 100 msec). Time constants changed as an exponential function of the membrane potential. I_{AB}, its time course, G_{AB}, and E_{AB} were not modified in the following conditions: (1) Na^+- and Ca^{2+}-free solutions, (2) intracellular EGTA, (3) extracellular (100 mM) or intracellular tetraethylammonium, (4) extracellular Cs^+ (up to 50 mM), Rb^+ (up to 10 mM), Ba^{2+} (13.5 mM), or Mn^{2+} (13.5 mM). However, low extracellular concentrations of Cd^{2+} or Zn^{2+} strongly and reversibly reduced both I_L and I_{AB}. Therefore, we conclude that anomalous rectification in crayfish muscle is generated by a voltage- and time-dependent K^+ current I_{AB}. This current displayed many electrophysiological and pharmacological characteristics that distinguished it from all others mediating anomalous rectification described previously.

[Key words: anomalous rectification, inward rectifier, hyperpolarization-activated current, K^+ current, Cd^{2+} blockade, crayfish muscle]

Katz (1949) reported a higher membrane conductance for inward than for outward current injection in frog skeletal muscle fibers. This nonlinear membrane behavior, termed anomalous or inward rectification, was later found with different characteristics in other systems. Two main varieties of conductances accounting for anomalous rectification have been described. (1) In frog skeletal muscle (Katz, 1949), cardiac muscle (Hall et al., 1963; Sakmann and Trube, 1984), metacerebral giant cells (Kandel and Tauc, 1966), marine eggs (Hagiwara and Takahashi, 1974), tunicate embryos (Miyazaki et al., 1974), and vertebrate neurons (Constanti and Galvan, 1983; Kaneko and Tachibana, 1985; Stanfield et al., 1985; Williams et al., 1988), anomalous rectification is mediated by K^+, and depends on the extracellular K^+ concentration ($[K^+]_o$), and its voltage dependence is a function of the difference between the membrane potential (V_m) and the potassium equilibrium potential (E_K) (Hagiwara and Takahashi, 1974; Hagiwara and Yoshii, 1979; Leech and Stanfield, 1981). It shows instantaneous voltage-dependent activation followed by a rapid time- and voltage-dependent component, and has been termed inward rectifying current. (2) Another type of inward rectification carried by Na^+ and K^+ was found in cardiac muscle (Brown and DiFrancesco, 1980; Yanagihara and Irisawa, 1980), hippocampal pyramidal neurons (Halliwell and Adams, 1982), and lobster slowly adapting stretch receptor neurons (Edman et al., 1987). This current, termed I_h, I_f, or I_q, was later found in several vertebrate neurons (Mayer and Westbrook, 1983; Spain et al., 1987; Takahashi, 1990) and was also called I_{AR} or I_{IR}. To differentiate it from the inward-rectifying current, it has been more generally called hyperpolarization-activated current. It has no instantaneous voltage-dependent component, shows considerably slower activation kinetics, and its activation is independent of $[K^+]_o$.

A third type of inward rectification carried by Cl^- has been reported in *Aplysia* neurons (Chesnoy-Marchais, 1983), amphibian oocytes (Parker and Miledi, 1988), and mammalian hippocampal neurons (e.g., Madison et al., 1986).

Fatt and Ginsborg (1958) described a delayed decrease in input resistance evoked by hyperpolarizing current pulses in crayfish muscle, but the underlying conductance had not been characterized under voltage clamp. Therefore, the aim of the present investigation was to characterize the current responsible for the anomalous rectification in crayfish muscle using the two-microelectrode voltage-clamp technique. This voltage- and time-dependent K^+ current shows no instantaneous component, thus we will call it hyperpolarization-activated current. However, it displayed many electrophysiological and pharmacological characteristics that distinguished it from all others described previously. Since this new hyperpolarization-activated current mediates anomalous rectification and probably acts as a K^+ balance by reestablishing the transmembrane K^+ concentration difference after prolonged activation of crayfish muscle, it will be named I_{AB}.

Received Apr. 5, 1993; revised July 7, 1993; accepted July 13, 1993.

We thank Drs. M. Gola and C. F. Stevens for critical reading of the manuscript. This work was supported by DGICYT and CEC grants to W.B. A.A. is a CajaMadrid fellow.

Correspondence should be addressed to Dr. Washington Buño, Neurofisiología, Instituto Cajal, Avenida Doctor Arce 37, E-28002 Madrid, Spain.

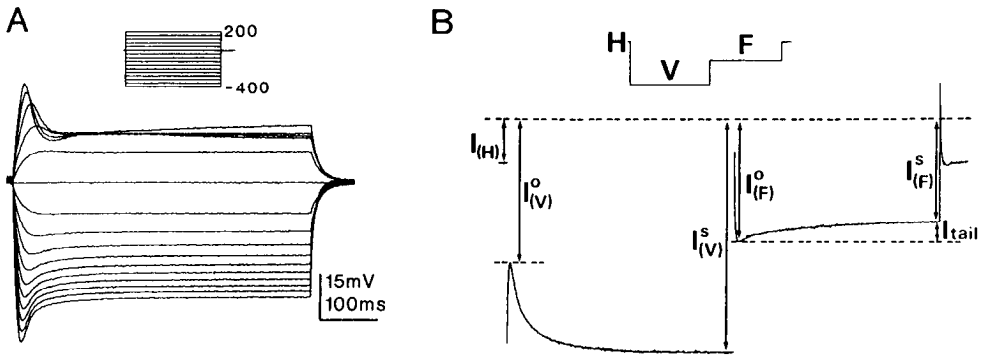

Figure 1. Anomalous rectification; conventions and parameters measured. *A*, Membrane potential responses (*bottom*) evoked by dehyperpolarizing current pulses (*top*); current-clamp condition. Schematic stimulus protocol with pulses to +200 nA and −400 nA, in 40 nA increments; resting potential (RP) was −65 mV. *B*, Currents (*lower*) evoked by two-pulse voltage command protocol (*upper*) with initial pulse (V) from the holding potential (H) and final pulse (F); voltage-clamp situation, as in all other figures. The currents evoked by H, V, and F were $I_{(H)}$, $I_{(V)}$, and $I_{(F)}$, respectively, and were measured from the zero current level (*upper broken line*). For each current, the superscripts 0 and S indicate the initial and steady state levels, respectively. I_{tail} was the $I^0_{(F)} - I^S_{(F)}$ difference.

A preliminary report of part of the present results has been published as a short communication (Araque and Buño, 1991).

Materials and Methods

Preparation. Opener muscles from the propodite of the first walking leg of crayfish (*Procambarus clarkii*) were isolated and transferred to a superfusion chamber (2 ml). Small crayfish (<5 cm) with short muscle fibers (<400 μm) were used for better space-clamp characteristics.

Microelectrodes and recordings. Fibers were impaled with two micropipettes usually filled with 1 M KCl (1–5 MΩ). When measuring the Cl^- equilibrium potential (E_{Cl}), micropipettes were filled with 3 M K-acetate (1–5 MΩ). In some experiments, the current electrode (filled with 1 M KCl) was substituted, after a control recording, by a new electrode filled either with 700 mM EGTA [ethyleneglycol-bis-(β-aminoethyl ether) N,N,N'N'-tetraacetic acid], neutralized with KOH (pH 7.2), or with 1 M tetraethylammonium chloride (TEA). EGTA and TEA were ionophoretically injected with 100 nA negative and positive current pulses, respectively, during 15 min. A 1 M KCl-agar Ag-AgCl electrode was used as the indifferent electrode. An Axoclamp-2A amplifier (Axon Instruments, Foster City, CA) was employed for two-electrode current- and voltage-clamp recordings. Probe gains in the voltage-clamp configuration were ×1 and ×10 for voltage and current electrodes, respectively. To decrease the coupling capacitance a grounded shield was constructed by coating one microelectrode with conductive paint. Voltage command pulses and injected currents were continuously monitored on a storage oscilloscope and stored on FM tape (0–1250 Hz bandwidth; Hewlett-Packard, model 3964a). The time required to reach the command pulse potential was ≤0.5 msec and there were no variations throughout the pulse. Capacitive currents ended within about 5 msec. Recordings that did not meet these criteria were rejected. The selected data were also sampled (Lab Master TM-40, Scientific Solutions Inc.), stored, and analyzed on an IBM PC/AT personal computer. Current records were sometimes filtered above 1 kHz with an active filter (Ithaco, model 4212).

Solutions. The normal solution, modified from Van Harreveld (1936), had the following composition (in mM): NaCl, 210; KCl, 5.4; $CaCl_2$, 13.5; $MgCl_2$, 2.6; Tris buffer, 10; pH adjusted to 7.2 with HCl. Test solutions were made with chloride salts of monovalent (Cs^+ and Rb^+) and divalent (Ba^{2+}, Mg^{2+}, Mn^{2+}, Cd^{2+}, and Zn^{2+}) cations, added in equimolar exchange with NaCl and $CaCl_2$, respectively. Ca^{2+}-free solutions were obtained by equimolar replacement of Ca^{2+} by Mg^{2+} and addition of 5 mM EGTA. TEA and Ca^{2+}-free TEA solutions were obtained by equimolar exchange of NaCl by 100 mM TEA in normal and Ca^{2+}-free solutions, respectively. In Na^+-free solutions, NaCl was replaced equimolarly by either choline chloride or Tris base (titrated with HCl). In experiments with increased $[K^+]_o$, KCl was either replaced to NaCl (or to Tris in Na^+-free solution) or was added without osmolarity compensation.

Each opener muscle fiber is innervated by a single inhibitory axon which releases γ-aminobutyric acid (GABA), evoking an increase in the postsynaptic membrane Cl^--conductance mediated by $GABA_A$ receptors (Takeuchi and Takeuchi, 1965, 1967). To test E_{Cl}, short (up to 250 msec) air pressure pulses delivered by a Picospritzer II (General Valve Corporation) were used to eject small quantities of 0.1 M GABA from a micropipette (tip diameter of 2–5 μm) placed over the fiber surface. Thus, E_{Cl} was estimated from the reversal potential of the GABA-induced postsynaptic currents. Experiments were performed at room temperature (21–23°C). All chemicals were purchased from Sigma.

Protocols and parameter measurements. Two voltage command protocols were used. They consisted of a pulse to an initial voltage (V) from a holding potential (H), followed by a pulse to a final voltage (F). In protocol 1, V was variable in amplitude and F was fixed. In protocol 2, V was constant and F was variable. A low-intensity, brief, final pulse was usually added to test for undue conductance changes (e.g., see Fig. 2*B*). A typical command pulse protocol and the evoked currents are illustrated in Figure 1*B*. The following conventions and current measurements were used throughout the text. (1) All currents were measured from the zero level (upper broken line). (2) The steady state current at the holding potential H was the holding current ($I_{(H)}$); in Figure 1*B* it was artificially increased for illustration purposes. (3) The initial pulse from H to V evoked an instantaneous current component ($I^0_{(V)}$) followed by a time-dependent current that reached a steady state ($I^S_{(V)}$). (4) The final pulse from V to F evoked an instantaneous current ($I^0_{(F)}$) and then a time-dependent current eventually reaching a steady state ($I^S_{(F)}$). (5) At any voltage, the hyperpolarization-activated inward current (I_{AB}) corresponded to the difference between the current at any time and the instantaneous current. Thus, the $I^S_{(V)} - I^0_{(V)}$ and $I^0_{(F)} - I^S_{(F)}$ differences corresponded to the steady state activation and deactivation of I_{AB} at V and F, respectively. All data are expressed as mean ± SD.

Results

This study is based on data from 127 opener muscle fibers. A representative sample of 31 fibers showed a resting membrane potential (RP) of −64.8 ± 5.8 mV and an input resistance of 0.4 ± 0.2 MΩ. Typical current-clamp responses evoked by hyperpolarizing and depolarizing pulses are shown in Figure 1*A*. Both small depolarizing and hyperpolarizing current pulses evoked passive responses. Higher-intensity depolarizing pulses elicited active graded responses. With higher-intensity hyperpolarizing currents, the membrane potential (V_m) attained an initial peak value at about 50 msec and then gradually decayed, reaching a steady state within about 500 msec. The steady state current versus V_m relationship showed a clear nonlinearity in the hyperpolarizing direction, indicating inward or anomalous rectification.

The ionic conductance responsible for the anomalous rectification was investigated under voltage clamp. In order to reduce

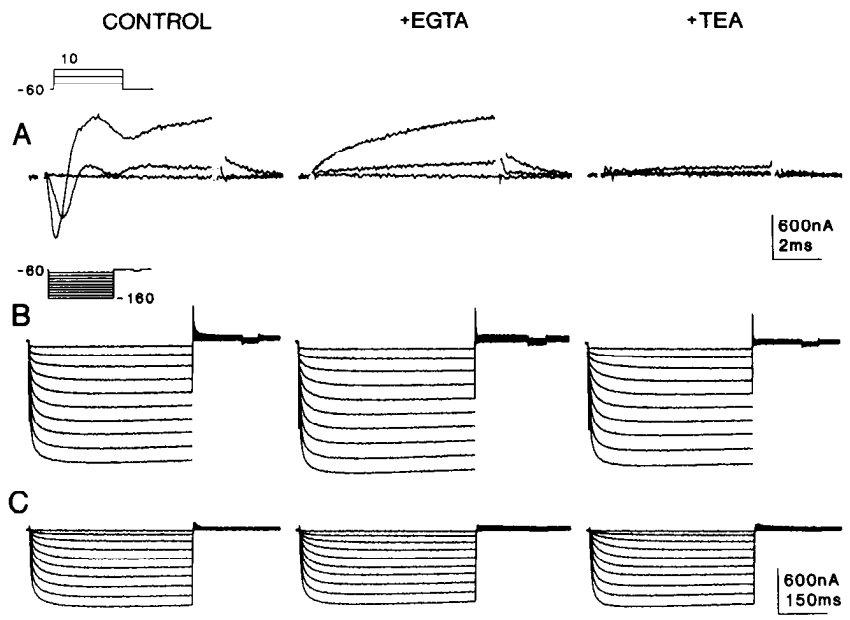

Figure 2. Currents evoked by voltage pulses in normal (control), Ca^{2+}-free (+EGTA), and Ca^{2+}-free TEA (+TEA) solutions. *A*, Depolarization-activated currents evoked by brief pulses from −60 to −40, −15, and 10 mV; linear currents were subtracted. *B*, Total inward currents activated by protocol 1 from $H = -60$ mV to $V = -160$ mV, in −10 mV increments (*top*, as in all figures). A brief, final, −5 mV pulse was added (as in most other cases) to test for unwanted conductance modifications. *C*, Same as *B*, but after subtraction of linear currents, showing voltage- and time-dependent current (I_{AB}). Current records were filtered at 1 kHz.

the holding current $I_{(H)}$ and to avoid activation of voltage-gated currents, fibers were clamped at $H = -60$ mV, near the RP. In solutions with raised $[K^+]_o$, H was set close to the attained RP. Figure 2*A* shows typical currents evoked by 11 msec duration depolarizing pulses from −60 to −40, −15, and 10 mV (the instantaneous linear currents were subtracted) in normal (control), Ca^{2+}-free (+EGTA), and Ca^{2+}-free TEA (+TEA) solutions. There is evidence indicating that the depolarization-activated currents shown in Figure 2*A* are an early inward Ca^{2+} current (I_{Ca}), an early Ca-dependent K^+ current ($I_{K(Ca)}$), and a late outward K^+ current (I_K) (Mounier and Vassort, 1975a,b; Hencek and Zachar, 1977; Hencek et al., 1978). Both I_{Ca} and $I_{K(Ca)}$ were suppressed in Ca^{2+}-free solution.

In Figure 2*B*, the 500-msec-duration hyperpolarizing command pulses from $H = -60$ mV to different V between −70 and −160 mV evoked an instantaneous current $I^0_{(V)}$ followed by a gradually developing inward current that reached a steady state $I^s_{(V)}$ within about 500 msec. Although both $I^0_{(V)}$ and $I^s_{(V)}$ increased with hyperpolarization, the latter increased more than the former. Since at any given voltage pulse $I^s_{(V)}$ was higher than $I^0_{(V)}$ (except the smallest pulse that did not activate the current), the time- and voltage-dependent inward current was associated with an increase in the membrane chord conductance (see Spain et al., 1987). Figure 2*C* shows the hyperpolarization-activated current (I_{AB}) in isolation, obtained by subtraction of the instantaneous linear components from the total inward current.

Figure 3 shows the current–voltage (*I–V*) relationships of the currents shown in Figure 2. Whereas I_{Ca} (solid triangles) was suppressed, I_K was unaffected in Ca^{2+}-free solution. The remaining I_K (solid circles above −60 mV) was strongly reduced when TEA was added. Both the steady state total inward current (open circles) and I_{AB} (i.e., $I_{AB} = I^s_{(V)} - I^0_{(V)}$: solid circles below −60 mV) were unchanged in Ca^{2+}-free and Ca^{2+}-free TEA solution. Similar results were obtained by intracellular injection of TEA (not shown), indicating that the I_{AB} channel has no extracellular or intracellular TEA sensitivity.

Instantaneous current–voltage relationships

Figure 4, *A* and *B*, exhibits voltage-clamp responses in Ca^{2+}-free TEA solution evoked by the protocols 1 and 2 used to measure the instantaneous on and off *I–V* relationships, respectively. $I^0_{(V)}$ and $I^0_{(F)}$ were measured 7 msec after the pulse transients, when the capacitive currents had ended, and the activation or deactivation of I_{AB} was negligible. Pulses > -100 mV were not used to measure $I^0_{(V)}$, because they evoked a significant amount of I_{AB} (see below). However, it is conceivable that $I^0_{(V)}$ remained linear beyond that value, as occurred in other fibers.

The *I–V* relation of $I^0_{(V)}$ obtained with pulses from $H = -60$ mV to V between −25 and −100 mV (Fig. 4*C*, triangles), was linear ($r > 0.99$). Therefore, the membrane did not exhibit instantaneous inward rectification, the instantaneous linear current obeyed Ohm's law, and it could be written as

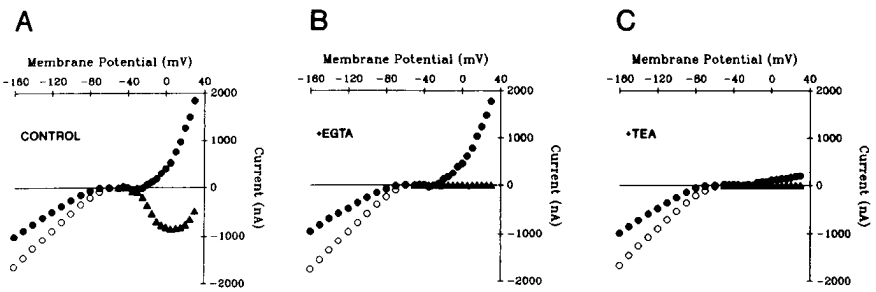

Figure 3. *I–V* relationships of currents recorded in normal (*A*), Ca^{2+}-free (*B*), and Ca^{2+}-free TEA (*C*) solutions. Data are from Figure 2. *Solid triangles*, peak inward Ca^{2+} current; *open circles*, $I^s_{(V)}$ evoked by hyperpolarizing pulses; *solid circles*, I_{AB} (under −60 mV) and late outward K^+ current (above −60 mV) measured at the end of the V pulse. *Open* and *solid symbols* indicate total currents and after subtraction of linear components, respectively.

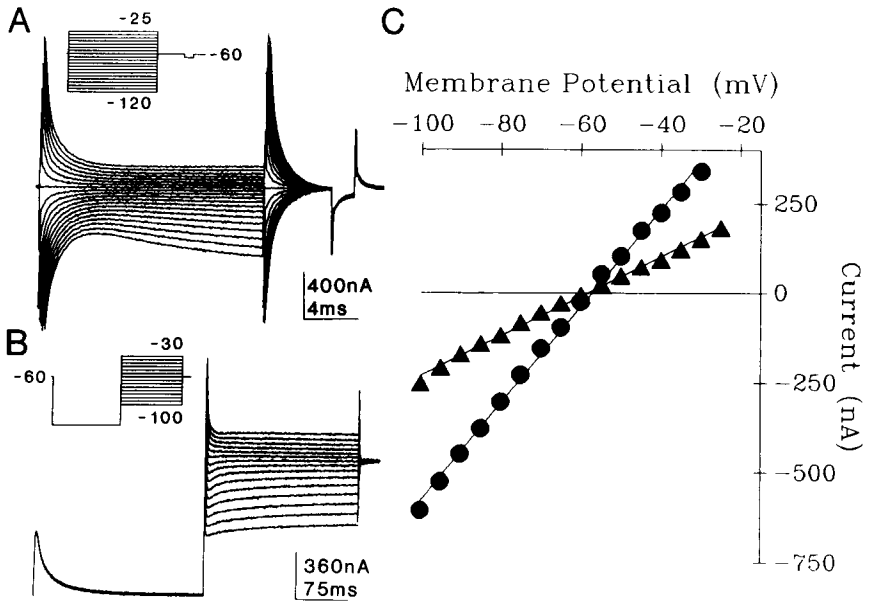

Figure 4. Instantaneous *I–V* relationships in Ca^{2+}-free TEA solution. *A*, Total currents evoked by protocol 1 from $H = -60$ mV to V from -25 to -120 mV, in -5 mV increments. *B*, Total currents in response to protocol 2 from $H = -60$ mV to $V = -130$ mV, followed by F from -30 to -100 mV, in -5 mV increments. *C*, *I–V* relationships of $I^0_{(I)}$ (*triangles*) and $I^0_{(F)}$ (*circles*) fitted to first-order regressions ($r > 0.99$) (*solid lines*).

$$I^0_{(I)} = I_L = G_L (V_m - E_L), \quad (1)$$

where G_L and E_L are the chord conductance and the reversal potential of the voltage-independent linear current I_L, respectively. Similarly, a linear relation was obtained for $I^0_{(F)}$ ($r > 0.99$) by stepping V_m from the V pulse at -130 mV to F from -30 to -100 mV (Fig. 4*C*, solid circles), indicating that the behavior of the total ionic current was also ohmic. Since both $I^0_{(I)}$ and $I^0_{(F)}$ obeyed Ohm's law, I_{AB} did so too, verifying the equation

$$I_{AB} = G_{AB} (V_m - E_{AB}), \quad (2)$$

where G_{AB} and E_{AB} were the chord conductance and the reversal potential of I_{AB}, respectively. Hence, the total ionic current (I_{total}) may be written as

$$I_{total} = I_L + I_{AB} = G_L (V_m - E_L) + G_{AB} (V_m - E_{AB}), \quad (3)$$

and I_{AB} could be unerringly isolated from I_{total} by subtraction of the linear, voltage-independent, current I_L.

The slopes of the linear regressions of the *I–V* relationships of $I^0_{(I)}$ and $I^0_{(F)}$ represented the resting chord conductance and the resting chord conductance plus G_{AB} at -130 mV, respectively. They were 5.5 and 13.5 μS, respectively, confirming that an increase in the membrane chord conductance underlies I_{AB}. The $I^0_{(I)}$ and $I^0_{(F)}$ *I–V* relationships intersect at E_{AB}, as can be deduced from Equation 3, verifying the value of E_{AB} estimated from the tail currents evoked by protocol 2 (see below). Indeed, the intersection point of the *I–V* curves in Figure 4*C* (-56.5 mV) agrees well with E_{AB} estimated by tail currents shown in Figure 6*C* (-53.2 mV), which were obtained from the same fiber.

Voltage dependence of G_{AB}

The voltage dependence of G_{AB} was characterized by a dimensionless activation parameter (N_∞), similar to the n_∞ and m_∞ parameters defined by Hodgkin and Huxley (1952b), which varied from 0 to 1 as G_{AB} varied from zero to its maximum value

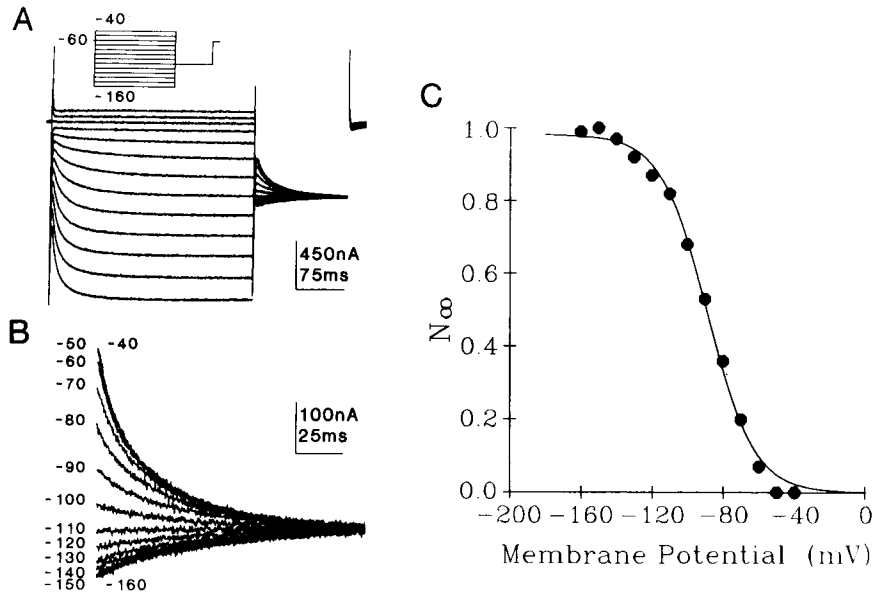

Figure 5. Voltage dependence of G_{AB}. *A*, Total membrane currents evoked by protocol 1 from $H = -60$ mV to V from -40 to -160 mV, in -10 mV increments, and to $F = -110$ mV. *B*, Expanded version of same tail currents. *C*, Activation curve of I_{AB}. N_∞ values were calculated from Equation 5 and fitted to the Boltzmann formalism (Eq. 6).

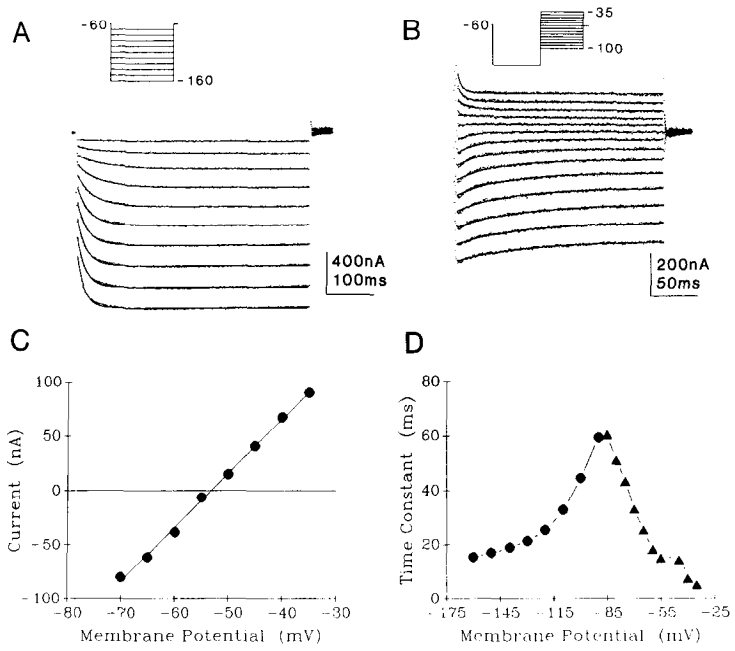

Figure 6. Reversal potential and time course of I_{AB}. *A*, Total currents (*dots*) elicited by protocol 1, from $H = -60$ mV to $V = -160$, in -10 mV increments, fitted with single-exponential functions ($r > 0.95$) (*solid lines*). *B*, Tail currents (*circles*) evoked by protocol 2, from $H = -60$ mV to $V = -170$ mV and F from -35 to -100 mV, in -5 mV increments, fitted with single-exponential functions ($r > 0.95$) (*solid lines*). *C*, Tail current amplitudes of I_{AB} versus membrane potential (V_m), fitted to a first order regression ($r > 0.99$) (*solid line*). *D*, I_{AB} activation (*circles*) and deactivation (*triangles*) time constants versus V_m.

($G_{AB,max}$), and which represents the steady state ensemble probability of I_{AB} channel activation; N_∞ was calculated from currents evoked by protocol 1 (Fig. 5*A*) with voltage command pulses from H to different V (usually from -40 to -160 mV) followed by an F pulse to a fixed value (usually -110 mV). Since F, E_{AB}, E_L, and G_L were constants, Equation 3 could be rewritten as

$$I^0_{(F)} = G_L (F - E_L) + G_{AB} (F - E_{AB}) = \beta + \alpha G_{AB}, \quad (4)$$

where α and β were constants. Thus, any change in G_{AB} will be reflected in $I^0_{(F)}$. $I^0_{(F)}$ had a minimum value ($I^0_{(F),min}$) when $G_{AB} = 0$ and it reached a maximum value ($I^0_{(F),max}$) when $G_{AB} = G_{AB,max}$. Therefore, N_∞ was defined as

$$N_\infty = (I^0_{(F)} - I^0_{(F),min}) / (I^0_{(F),max} - I^0_{(F),min}). \quad (5)$$

Figure 5*C* shows the N_∞ versus V_m relation or activation curve of I_{AB}. The data obtained were fitted to the expression

$$N_\infty = \tilde{N}_\infty [1 + \exp(V - V_0)/S]^{-1}, \quad (6)$$

deduced from the Boltzmann equation, where $\tilde{N}_\infty$ is the limiting activation parameter (usually equal to 1), V_0 the voltage at which G_{AB} is half-activated, and S a slope parameter.

Results obtained from 17 muscle fibers indicate that the activation of G_{AB} increased sigmoidally with hyperpolarization, started close to the RP, and could be fitted ($r > 0.99$) with the Boltzmann equation. The voltage dependence showed a mean half-activation at -94.4 ± 7.1 mV, a slope factor of 12.4 ± 2.7, and a $G_{AB,max} = 7.8 \pm 3.6$ μS. N_∞ approached unity at -130 mV and usually saturated at $V_m > -140$ mV. Hyperpolarization beyond about -140 mV sometimes evoked a large, slow, long-lasting inward current, probably due to membrane breakdown. Thus, strong hyperpolarizations were employed only when this current was not present.

Kinetic behavior of I_{AB}

The time course of both I_{AB} activation and deactivation (i.e., during the V and F pulses, Fig. 6, *A* and *B*, respectively) could be fitted ($r > 0.95$) by single-exponential functions of the form

$$I_{AB(I)} = a + b \exp(-t/\tau_{on}),$$
$$I_{AB(F)} = c + d \exp(-t/\tau_{off}),$$

where a, b, c, and d were constants and τ_{on} and τ_{off} were the activation and deactivation time constants, respectively. While τ_{on} decreased with increasing hyperpolarization (Fig. 6*D*, circles), declining e-fold for 23.6 mV, τ_{off} decreased e-fold every 31.7 mV with depolarization (Fig. 6*D*, triangles), both being exponential functions of V_m. The similarity of τ_{on} and τ_{off} magnitudes indicates that both the I_{AB} activation and deactivation kinetics may be described by a single time constant (τ_{AB}). For convenience, τ_{AB} corresponded to τ_{on} for relatively large hyperpolarizations, whereas it corresponded to τ_{off} for the remaining voltages.

According to what is deduced from Hodgkin and Huxley (1952a), the time constant of voltage-gated currents with an activation curve like that of I_{AB} should be bell-shaped functions of V_m with a peak at the half-activation voltage V_0 (see also Mayer and Westbrook, 1983). Figure 6*D* shows that τ_{AB} was a bell-shaped function of V_m with a peak around V_0 (compare with Fig. 5, same fiber).

Ionic nature of I_{AB}

The reversal potential of I_{AB} was estimated from the reversal potential of tail currents evoked by protocol 2. Figure 6*B* shows the expanded tail currents in Figure 4*B*. Since the fully activated I_{AB} did not exhibit rectification and its deactivation was time dependent, then

$$I_{tail} = I^0_{(F)} - I^s_{(F)} = \Delta G_{(F)} (F - E_{AB}), \quad (7)$$

where $\Delta G_{(F)}$ is the difference between the conductance at the beginning and at the end of the F pulse. Figure 6*C* shows the I–V relation of I_{tail} from Figure 6*B* and the corresponding first-order regression fit ($r > 0.99$). The reversal potential of I_{AB} estimated by linear interpolation was -53.2 mV. The mean value of E_{AB} was -61.8 ± 6.3 mV ($n = 28$), which did not differ substantially from the average RP.

Effects of Ca^{2+}. The effects of Ca^{2+}-free solutions and of in-

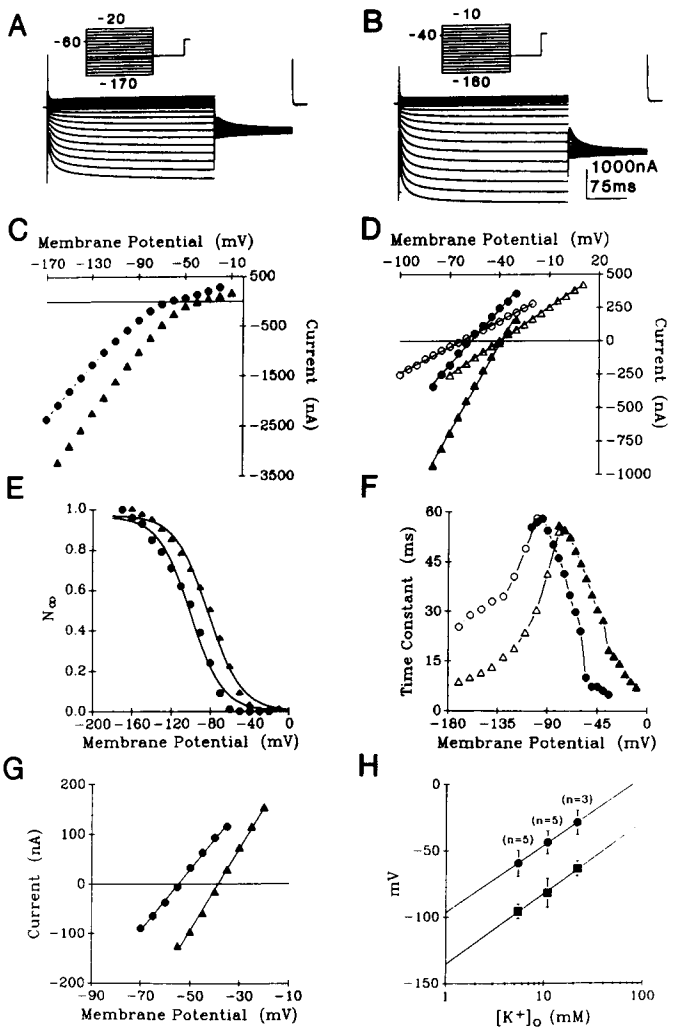

Figure 7. Effects of increased $[K^+]_o$ on I_{AB}. *A* and *B*, Total currents evoked in 5.4 mM $[K^+]_o$ and 10.8 mM $[K^+]_o$, respectively, in Ca^{2+}-free solution. Protocol 1, with $H = -60$ mV for *A* and $H = -40$ mV for *B*, respectively. *C–G*, *Circles* and *triangles* correspond to 5.4 mM and 10.8 mM $[K^+]_o$, respectively. *C*, *I–V* relationships of $I^s_{(t)}$. *D*, *I–V* relations of $I^0_{(t)}$ and $I^0_{(f)}$ (*open* and *solid symbols*, respectively), fitted by first-order regressions ($r > 0.99$) (*solid lines*). *E*, Activation curves. N_∞ values were obtained from Equation 5 and fitted to Equation 6. *F*, τ-V_m relationships of the activation (*open symbols*) and deactivation (*solid symbols*). *G*, Tail current amplitudes of I_{AB} versus V_m. Tail currents were evoked by protocol 2. *H*, Semilogarithmic plot of E_{AB} (*circles*) and mean half-activation of G_{AB} (*squares*) in different $[K^+]_o$, fitted by first-order regressions ($r > 0.99$); n = number of fibers.

ternal injection of EGTA were tested. I_{AB}, its kinetics, E_{AB}, and G_{AB} were not significantly modified in Ca^{2+}-free solution or by intracellular EGTA (Figs. 2, 3, 7), suggesting that neither extracellular nor intracellular Ca^{2+} contributes to I_{AB}.

Effects of Na^+ substitutions. Total replacement of NaCl by either Tris or choline chloride did not evoke any modification of I_{AB}, τ_{AB}, E_{AB}, or G_{AB}, indicating that Na^+ did not contribute to I_{AB} and that its activation was unaffected by Na^+ (data not shown).

Consequences of $[K^+]_o$ modifications. The average RP, measured in five fibers, shifted toward positive potentials by 57.6 mV for a 10-fold change in $[K^+]_o$. Indeed, when $[K^+]_o$ was increased from 5.4 to 10.8 and 21.6 mM, the RP shifted from -61.5 ± 3.8 ($n = 5$) to -40.7 ± 5.5 ($n = 5$) and -26.8 ± 5.8 mV ($n = 3$), respectively. Figure 7, *A* and *B* shows currents evoked by protocol 1 in Ca^{2+}-free TEA solution with 5.4 mM and 10.8 mM $[K^+]_o$, respectively. The *I–V* relationship of $I^s_{(t)}$ (Fig. 7*C*), and of the instantaneous currents $I^0_{(t)}$ and $I^0_{(f)}$ (Fig. 7*D*, open and solid symbols, respectively), shifted to the right in high $[K^+]_o$. Moreover, the slope of the *I–V* relation of $I^0_{(t)}$ or resting chord conductance at each H augmented on the average 1.4 ± 0.1 times in raised $[K^+]_o$ (e.g., Fig. 7*D*, open symbols). Contrastingly, $G_{AB,max}$ did not change significantly.

The I_{AB} activation curve also shifted to the right in doubled $[K^+]_o$ (Fig. 7*E*). The half-activation potential V_0 varied from -100.0 to -81.9 mV while S slightly changed from 16.4 to 17.0 in 5.4 mM (circles) and 10.8 mM (triangles), respectively. On the average, V_0 changed 53.6 mV ($r > 0.99$) with a 10-fold increase in $[K^+]_o$ (Fig. 7*H*, squares). Therefore, the I_{AB} activation depends on the $V_m - E_K$ difference.

The magnitude of τ_{AB} was not modified by increasing $[K^+]_o$, but its voltage dependence was changed, shifting the relation between τ_{AB} and V_m toward positive potentials, as expected by the change in the activation curve. Indeed, the peak of the bell-shaped curve was displaced 18 mV to the right in raised $[K^+]_o$ (Fig. 7*F*).

E_{AB} estimated from the tail currents (protocol 2) changed from -54.7 to -38.6 mV when $[K^+]_o$ was raised (Fig. 7*G*, circles and triangles, respectively). On the average, E_{AB} shifted toward positive potentials by 50.8 mV for a 10-fold increase in $[K^+]_o$ (Fig. 7*H*, circles). Therefore, E_{AB} varied close to the Nernst prediction for a K^+ electrode (assuming an invariant intracellular K^+ concentration, $[K^+]_i$), and we can conclude that I_{AB} was selectively mediated by K^+. The surprisingly low E_K values are not unexpected according to similar results obtained from other crustacean muscles (see, e.g., Mounier and Vassort, 1975a; Hencek et al., 1978).

Although it has been firmly established that alterations of $[K^+]_o$ result in a rapid redistribution of Cl^- across the cell membrane in many systems, Boistel and Fatt (1958) showed no important E_{Cl} changes in raised $[K^+]_o$ and Cl^--free solution in crayfish opener muscle fibers. Their observations were based on inhibitory postsynaptic potential amplitude measurements made within the initial 15 min after the solution change and therefore do not preclude slower changes. Figure 8 shows the effects of raised $[K^+]_o$ on E_{AB}, the I_K reversal potential, and E_{Cl}. While the reversal potential of I_K and E_{AB} shifted from -60.1 and -63.5 to -46.5 and -49.4 mV, respectively, E_{Cl} did not change much (from -53.3 to -55.8 mV), in 5.4 and 10.8 mM $[K^+]_o$, respectively. I_{Cl} was the difference between $I^0_{(t)}$ with and without GABA (see Materials and Methods), and E_{Cl} was the reversal potential of I_{Cl}.

Our results are in close agreement with Boistel and Fatt (1958) since they indicate either little Cl^- redistribution or an extremely slow effect following $[K^+]_o$ changes.

Therefore, we can conclude that the actions of raised $[K^+]_o$ were not due to redistribution of Cl^-, and that I_{AB} was selectively carried by K^+.

Effects of monovalent cations Cs^+ and Rb^+

It is strongly established that low extracellular Cs^+ concentrations block both the inward-rectifying (Hagiwara et al., 1976; Gay and Stanfield, 1977) and the hyperpolarization-activated currents (DiFrancesco and Ojeda, 1980; Halliwell and Adams, 1982; Mayer and Westbrook, 1983; Spain et al., 1987; Takahashi, 1990). However, I_{AB} was unaffected by different Cs^+ con-

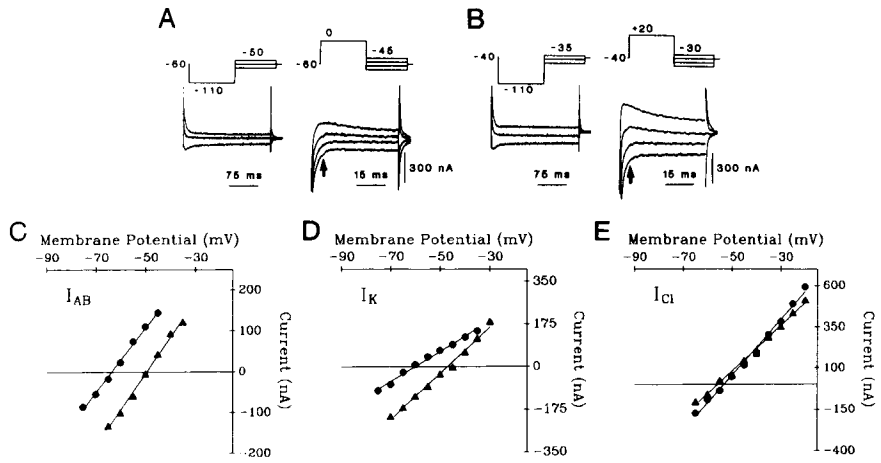

Figure 8. Effects of increased $[K^+]_o$ on E_{AB}, the I_K reversal potential, and E_{Cl} in Ca^{2+}-free solution. *A* and *B*, Tail currents of I_{AB} (*left*) and I_K (*right*) evoked in 5.4 and 10.8 mM $[K^+]_o$, respectively. *C* and *D*, Tail amplitudes of I_{AB} and I_K (measured at *arrows* in *A* and *B*), respectively, versus V_m. *E*, *I–V* relationships of the difference between $I^0_{(t)}$ with and without GABA. *Circles* and *triangles*, 5.4 and 10.8 mM $[K^+]_o$, respectively, fitted to first-order regressions ($r > 0.99$) (*solid lines*).

centrations (up to 50 mM). On the other hand, Rb^+ interacts with K^+-permeable channels in several tissues including both types of cationic inward rectifiers (Hagiwara and Takahashi, 1974; Standen and Stanfield, 1980; DiFrancesco, 1982), which are blocked by low concentrations of Rb^+ (under 10 mM). Nevertheless, the extracellular addition of 10 mM Rb^+ did not change I_{AB} (not shown).

Effects of divalent cations

Ba^{2+}, Mg^{2+}, and Mn^{2+}. Low concentrations of Ba^{2+} are known to block the inward-rectifying currents (10–100 μM; Hagiwara et al., 1978) but not the hyperpolarization-activated currents (Yanagihara and Irisawa, 1980; Halliwell and Adams, 1982; Mayer and Westbrook, 1983; Takahashi, 1990). When extracellular $CaCl_2$ was equimolarly replaced by $BaCl_2$, I_{AB} was not modified. I_{AB} was also unchanged when $CaCl_2$ was replaced either by $MgCl_2$ or $MnCl_2$, while the depolarization-activated inward Ca^{2+} current was totally suppressed in those conditions.

Action of Cd^{2+} and Zn^{2+}. The effects of 5 mM extracellular Cd^{2+} are shown in Figure 9*A*. Low extracellular Cd^{2+} concentrations (<5 mM) strongly and reversibly reduced both I_{AB} and the instantaneous linear current (Fig. 9, *B* and *C*, respectively), while the holding current $I_{(H)}$ was not significantly affected. Similar results were obtained with millimolar extracellular Zn^{2+} concentrations (Fig. 10). The effects of Cd^{2+} and Zn^{2+} on I_{AB} were dose dependent, both with an IC_{50} of about 300 μM (A. Araque, D. Cattaert, and W. Buño, unpublished observations). It is noteworthy that the anomalous rectification observed with hyperpolarizing pulses in current-clamp conditions was also suppressed by Cd^{2+} and Zn^{2+} (not shown).

Discussion

The above-described experiments indicate that a hyperpolarization-activated time-dependent inward K^+ current I_{AB} operates in opener muscle fibers of crayfish. This current underlies the inward (i.e., anomalous) rectification existing in current-clamp conditions (Fig. 1*A*). Although the effects of I_{AB} activation were similar to those of other inward-rectifying and hyperpolarization-activated currents, I_{AB} displayed many electrophysiological and pharmacological characteristics that distinguished it from all others previously described.

There are two main varieties of currents accounting for inward rectification in neurons, muscle fibers, and oocytes (see introductory remarks): first, a K^+ current that has a characteristic

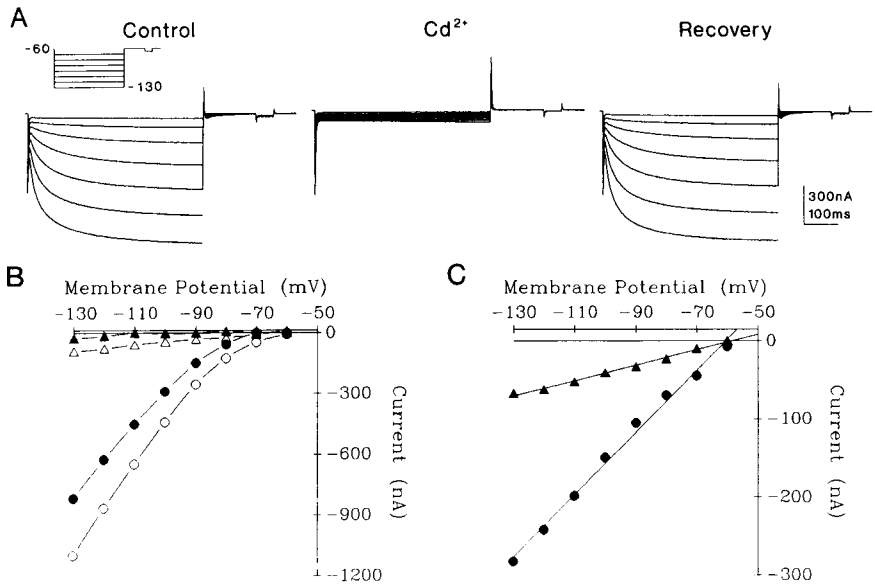

Figure 9. Effects of extracellular Cd^{2+}. *A*, Total inward currents evoked by protocol 1, from $H = -60$ to $V = -130$ mV, in −10 mV increments, in normal solution (control), 5 mM Cd^{2+}, and recovery after washout. *B*, *I–V* relationships of $I^s_{(t)}$ (*open symbols*) and I_{AB} (*solid symbols*) in normal (*circles*) and 5 mM Cd^{2+} (*triangles*) solutions. *C*, *I–V* relations of $I^0_{(t)}$ in normal (*circles*) and 5 mM Cd^{2+} (*triangles*) solutions, fitted by first-order regressions ($r > 0.99$).

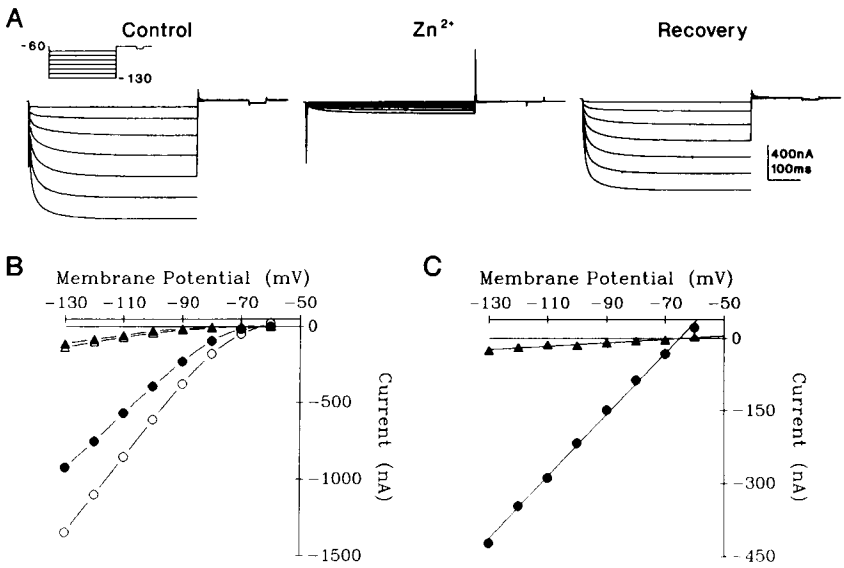

Figure 10. Effects of extracellular Zn^{2+}. *A–C* are as in Figure 9, but with 3 mM Zn^{2+}. *B*, *I–V* relationships of $I^{s}_{(t)}$ (*open symbols*) and I_{AB} (*solid symbols*) in normal (*circles*) and 3 mM Zn^{2+} (*triangles*) solutions. *C*, *I–V* relations of $I^{0}_{(t)}$ in normal (*circles*) and 3 mM Zn^{2+} (*triangles*) solutions, fitted by first-order regressions ($r > 0.99$).

instantaneous voltage-dependent component followed by a rapid voltage- and time-dependent element—its conductance is a function of $[K^+]_o$, and has an activation curve that is contingent on the $V_m - E_K$ difference (e.g., Hagiwara and Takahashi, 1974; Hagiwara and Yoshii, 1979; Leech and Stanfield, 1981); and second, a slower time-dependent hyperpolarization-activated current termed I_h, I_f, or I_q, carried by Na^+ and K^+. It lacks the instantaneous voltage-dependent component, and its activation is independent of $[K^+]_o$ (Brown and DiFrancesco, 1980; Yanagihara and Irisawa, 1980; Halliwell and Adams, 1982; Edman et al., 1987).

Two different mechanisms have been proposed to explain both current types. The hyperpolarization-activated currents are pictured as due to the intrinsic voltage-sensitive gating mechanisms of channels that when open are ohmic. On the other hand, the instantaneous voltage-dependent component of the inward-rectifying current is represented as generated by the rectifying quality of the open channels themselves (Sakmann and Trube, 1984), without the participation of intrinsic gating mechanisms. Evidence exists indicating that intracellular Mg^{2+}, at physiological concentrations, acts as the voltage-dependent blocker that grants instantaneous rectification to the otherwise ohmic open channels (Matsuda et al., 1987; Matsuda, 1991). However, the time-dependent component of the inward rectifier can also be explained by a gating mechanism (Hagiwara et al., 1976; Hagiwara and Yoshii, 1979; Leech and Stanfield, 1981). If such a gating mechanism also accounts for the instantaneous current component is still questionable (Ishihara et al., 1989; Silver and DeCoursey, 1990; Matsuda, 1991; Mitra and Morad, 1991).

In crayfish opener muscle fibers, the instantaneous current was voltage independent and displayed a linear *I–V* relationship; hence it could be the leak current I_L. Therefore, opener muscle fibers lack the instantaneous voltage-dependent component that is characteristic of inward-rectifying currents (see the references above). The activation of I_{AB} was time dependent, suggesting that rectification was due to the channel's kinetic characteristics. At a fixed degree of activation I_{AB} itself obeyed Ohm's law; therefore, rectification was not due to the attributes of the ohmic open channel. The time dependence of I_{AB} also implies that a gating mechanism is responsible for its activation.

Since the activation and the deactivation kinetics of I_{AB} were the same, the simplest representation to explain the above described phenomena—if an ohmic open channel with an intrinsic gating mechanism is assumed—is a two-state model like the one proposed by Chesnoy-Marchais (1983) to explain inward rectification carried by Cl^- in *Aplysia* neurons. Interestingly, this seems to be the only electrophysiological similarity between I_{AB} and the hyperpolarization-activated Cl^- current described by Chesnoy-Marchais (1983). Indeed, this current is carried by Cl^-, its activation curve depends on $[Cl^-]_i$, and its time course is relatively slow (with time constant in the second range). Contrastingly, I_{AB} is carried by K^+, its activation curve depends on $[K^+]_o$ and does not depend on $[Cl^-]_i$ (not shown), and its time course is faster (with a time constant at least two orders of magnitude lower).

Approximating the inward-rectifying K^+ currents (Hagiwara and Takahashi, 1974; Hagiwara and Yoshii, 1979; Leech and Stanfield, 1981), I_{AB} was specifically mediated by K^+, and the voltage dependence of its activation curve was a function of the $V_m - E_K$ difference. On the other hand, the conductance of the inward rectifier of marine oocytes is proportional to the square root of $[K^+]_o$ (Hagiwara and Yoshii, 1979). However, the conductance underlying I_{AB} was independent of $[K^+]_o$. Contrastingly, the leak conductance increased 1.4 ± 0.1 times in doubled $[K^+]_o$. Although the conductance of other hyperpolarization-activated currents (e.g., Mayer and Westbrook, 1983; Spain et al., 1987) increased in raised $[K^+]_o$, the hyperpolarization-activated current in rat spinal motoneurons did not display a similar behavior (Takahashi, 1990).

Although the electrophysiological characteristics of I_{AB} partially overlap with those of the other types of cationic inward rectification (see Discussion above), the prominent dissimilarity was the pharmacological sensitivity to different extracellular ions. Indeed, while the inward-rectifying currents are blocked by low concentrations of Ba^{2+} (0.01–5 mM, Standen and Stanfield, 1978; 10–100 μM, Hagiwara et al., 1978; 500 μM, Constanti and Galvan, 1983), I_{AB} was not altered in the presence of 13.5 mM Ba^{2+}. On the other hand, low concentrations of extracellular Cs^+ are known to block both the inward-rectifying (0.5–1 mM, Hagiwara et al., 1976; 2.5 mM, Gay and Stanfield, 1977) and the hyperpolarization-activated currents (20 mM, DiFrancesco

and Ojeda, 1980; 0.5–3 mM, Halliwell and Adams, 1982; 1–10 mM, Mayer and Westbrook, 1983; 2 mM, Takahashi, 1990); however, concentrations of Cs^+ up to 50 mM did not modify I_{AB}. Furthermore, I_{AB} was not modified by extracellular addition of 10 mM Rb^+, although this ion blocks the other cationic inward rectifications at concentrations under 10 mM (Hagiwara and Takahashi, 1974; Standen and Stanfield, 1980; DiFrancesco, 1982). Contrastingly, I_{AB} was blocked by the application of low concentrations of extracellular Cd^{2+} and Zn^{2+}.

In conclusion, our results provide evidence of the existence of a new type of voltage- and time-dependent inward rectification, selectively mediated by K^+, whose activation curve depends on $V_m - E_K$ (assuming a fixed $[K^+]_i$) but whose conductance is unaffected by $[K^+]_o$. It is blocked by low concentrations of Cd^{2+} and Zn^{2+} but is insensitive to other ions that are potent blockers of other inward rectifications; that is, Cs^+, Ba^{2+}, and Rb^+.

Although we can only speculate about the functional meaning of I_{AB}, the following possibilities are likely besides the K^+ balance function described above. E_{AB} is close to the RP; therefore, I_{AB} could stabilize the membrane potential preventing large hyperpolarizations. This function may be important in this muscle where hyperpolarizations due to postsynaptic inhibition are present (Takeuchi and Takeuchi, 1965, 1967). It is conceivable that owing to its voltage sensitivity and kinetics, I_{AB} could also modulate synaptic efficacy. The synaptic transmitters or modulators operative in this system could control its excitable behavior and the synaptic integration at the postsynaptic membrane through the activation or suppression of I_{AB}. Interestingly, we have found that I_{AB} was markedly increased by the crustacean neuromodulator octopamine (A. Araque and W. Buño, unpublished observations).

References

Araque A, Buño W (1991) Novel inward rectifier blocked by Cd^{2+} in crayfish muscle. Brain Res 563:321–324.

Boistel J, Fatt P (1958) Membrane permeability change during inhibitory transmitter action in crustacean muscle. J Physiol (Lond) 144: 176–191.

Brown HF, DiFrancesco D (1980) Voltage-clamp investigations of membrane currents underlying pace-maker activity in rabbit sino-atrial node. J Physiol (Lond) 308:335–351.

Chesnoy-Marchais D (1983) Characterization of a chloride conductance activated by hyperpolarization in *Aplysia* neurones. J Physiol (Lond) 342:277–308.

Constanti A, Galvan M (1983) Fast inward-rectifying current accounts for anomalous rectification in olfactory cortex neurones. J Physiol (Lond) 335:153–178.

DiFrancesco D (1982) Block and activation of the pace-maker channel in calf Purkinje fibres: effects of potassium, caesium and rubidium. J Physiol (Lond) 329:485–507.

DiFrancesco D, Ojeda C (1980) Properties of the current I_f in the sinoatrial node of the rabbit compared with those of the current I_{K2} in Purkinje fibres. J Physiol (Lond) 308:353–367.

Edman A, Gestrelius S, Grammp W (1987) Current activation by membrane hyperpolarization in the slowly adapting lobster stretch receptor neurone. J Physiol (Lond) 384:671–690.

Fatt P, Ginsborg BL (1958) The ionic requirements for the production of action potentials in crustacean muscle fibres. J Physiol (Lond) 142: 516–543.

Gay LA, Stanfield PR (1977) Cs^+ causes a voltage-dependent block of inward K currents in resting skeletal muscle fibres. Nature 267: 169–170.

Hagiwara S, Takahashi K (1974) The anomalous rectification and cation selectivity of the membrane of a starfish egg cell. J Membr Biol 18:61–80.

Hagiwara S, Yoshii M (1979) Effects of internal potassium and sodium on the anomalous rectification of the starfish egg as examined by internal perfusion. J Physiol (Lond) 292:251–265.

Hagiwara S, Miyazaki S, Rosenthal NP (1976) Potassium current and the effect of cesium on this current during anomalous rectification of the egg cell membrane of a starfish. J Gen Physiol 67:621–638.

Hagiwara S, Miyazaki S, Moody W, Patlak J (1978) Blocking effects of barium and hydrogen ions on the potassium current during anomalous rectification in the starfish egg. J Physiol (Lond) 279:167–185.

Hall AE, Hutter OF, Noble D (1963) Current–voltage relations of Purkinje fibres in sodium-deficient solutions. J Physiol (Lond) 166: 225–240.

Halliwell JV, Adams PR (1982) Voltage-clamp analysis of muscarinic excitation in hippocampal neurons. Brain Res 250:71–92.

Hencek M, Zachar J (1977) Calcium currents and conductances in the muscle membrane of the crayfish. J Physiol (Lond) 268:51–71.

Hencek M, Zachar J, Zacharova D (1978) Membrane currents in a calcium type muscle membrane under voltage clamp. Physiol Bohemoslov 27:457–466.

Hodgkin AL, Huxley AF (1952a) The components of membrane conductance in the giant axon of *Loligo*. J Physiol (Lond) 116:473–496.

Hodgkin AL, Huxley AF (1952b) A quantitative description of membrane current and its application to conduction and excitation in nerve. J Physiol (Lond) 117:500–544.

Ishihara K, Mitsuiye T, Noma A, Takano M (1989) The Mg^{2+} block and gating underlying inward rectification of the K^+ current in guinea-pig cardiac myocytes. J Physiol (Lond) 419:297–320.

Kandel ER, Tauc L (1966) Anomalous rectification in the metacerebral giant cells and its consequences for synaptic transmission. J Physiol (Lond) 183:287–304.

Kaneko A, Tachibana M (1985) Effects of L-glutamate on the anomalous rectifier potassium current in horizontal cells of *Carassius auratus* retina. J Physiol (Lond) 358:169–182.

Katz B (1949) Les constantes électriques de la membrane du muscle. Arch Sci Physiol 3:285–300.

Leech CA, Stanfield PR (1981) Inward rectification in frog skeletal muscle fibres and its dependence on membrane potential and external potassium. J Physiol (Lond) 319:295–309.

Madison DV, Malenka RC, Nicoll RA (1986) Phorbol esters block a voltage-sensitive chloride current in hippocampal pyramidal cells. Nature 321:695–697.

Matsuda H (1991) Magnesium gating of the inwardly rectifying K^+ channel. Annu Rev Physiol 53:289–298.

Matsuda H, Saigusa A, Irisawa H (1987) Ohmic conductance through the inwardly rectifying K^+ channel and blocking by internal Mg^{2+} Nature 325:156–159.

Mayer ML, Westbrook GL (1983) A voltage-clamp analysis of inward (anomalous) rectification in mouse spinal sensory ganglion neurones. J Physiol (Lond) 340:19–45.

Mitra R, Morad M (1991) Permeance of Cs^+ and Rb^+ through the inwardly rectifying K^+ channel in guinea-pig ventricular myocytes. J Membr Biol 122:33–42.

Miyazaki S, Takahashi K, Tsuda K, Yoshii M (1974) Analysis of non-linearity observed in the current–voltage relation of the tunicate embryo. J Physiol (Lond) 238:55–77.

Mounier Y, Vassort G (1975a) Initial and delayed membrane currents in crab muscle fibre under voltage-clamp conditions. J Physiol (Lond) 251:589–608.

Mounier Y, Vassort G (1975b) Evidence for a transient potassium membrane current dependent on calcium influx in crab muscle fibre. J Physiol (Lond) 251:609–625.

Parker I, Miledi R (1988) A calcium-independent chloride current activated by hyperpolarization in *Xenopus* oocytes. Proc R Soc Lond [Biol] 223:191–199.

Sakmann B, Trube G (1984) Conductance properties of single inwardly rectifying potassium channels in ventricular cells from guinea-pig heart. J Physiol (Lond) 347:641–657.

Silver M, DeCoursey TE (1990) Intrinsic gating of the inward rectifier in bovine pulmonary artery endothelial cells in the presence or absence of internal Mg^{2+}. J Gen Physiol 96:109–133.

Spain WJ, Schwindt PC, Crill WE (1987) Anomalous rectification in neurons from cat sensorimotor cortex *in vitro*. J Neurophysiol 57: 1555–1576.

Standen NB, Stanfield PR (1980) Rubidium block and rubidium permeability of the inward rectifier of frog skeletal muscle fibres. J Physiol (Lond) 304:415–435.

Stanfield PR, Nakajima Y, Yamaguchi K (1985) Substance P raises neuronal membrane excitability by reducing inward rectification. Nature 315:498–501.

Takahashi T (1990) Inward rectification in neonatal rat spinal motoneurones. J Physiol (Lond) 423:47–62.

Takeuchi A, Takeuchi N (1965) Localized action of gamma-aminobutyric acid on the crayfish muscle. J Physiol (Lond) 177:225–238.

Takeuchi A, Takeuchi N (1967) Anion permeability of the inhibitory post-synaptic membrane of the crayfish neuromuscular junction. J Physiol (Lond) 191:575–590.

Van Harreveld A (1936) A physiological solution for fresh water crustaceans. Proc Soc Exp Biol Med 34:428–432.

Williams JT, Colmers WF, Pan ZZ (1988) Voltage- and ligand-activated inwardly rectifying currents in dorsal raphe neurons *in vitro*. J Neurosci 8:3499–3506.

Yanagihara K, Irisawa H (1980) Inward current activated during hyperpolarization in the rabbit sinoatrial node cell. Pfluegers Arch 385: 11–19.